



OPEN

Asymmetric host movement reshapes local disease dynamics in metapopulations

Matthew Michalska-Smith^{1,2✉}, Kimberly VanderWaal¹ & Meggan E. Craft^{1,3}

Understanding how the movement of individuals affects disease dynamics is critical to accurately predicting and responding to the spread of disease in an increasingly interconnected world. In particular, it is not yet known how movement between patches affects local disease dynamics (e.g., whether pathogen prevalence remains steady or oscillates through time). Considering a set of small, archetypal metapopulations, we find three surprisingly simple patterns emerge in local disease dynamics following the introduction of movement between patches: (1) movement between identical patches with cyclical pathogen prevalence dampens oscillations in the destination while increasing synchrony between patches; (2) when patches differ from one another in the absence of movement, adding movement allows dynamics to propagate between patches, alternatively stabilizing or destabilizing dynamics in the destination based on the dynamics at the origin; and (3) it is easier for movement to induce cyclical dynamics than to induce a steady-state. Considering these archetypal networks (and the patterns they exemplify) as building blocks of larger, more realistically complex metapopulations provides an avenue for novel insights into the role of host movement on disease dynamics. Moreover, this work demonstrates a framework for future predictive modelling of disease spread in real populations.

Many populations of humans, livestock, and wildlife are comprised of densely occupied subpopulations, or “patches”, connected by the movement of individuals, i.e., a metapopulation. Most of the world’s population lives in cities¹, livestock are clustered on farms², and wildlife tend to cluster in space, especially when usable habitat is fragmented^{3,4}. For humans, movement between patches was once at such a low level that emerging diseases tended to be geographically constrained to the patch where they originated⁵. For instance, the strain of *Yersinia pestis* that resulted in The Black Death, was constrained to Europe for nearly four centuries before being introduced in China⁶. Likewise, Smallpox remained relatively isolated in subpopulations around Europe until the Crusades of the 11th and 13th centuries made it endemic across the continent, and it took until the 16th century for the pathogen to tag along colonizing expeditions the Americas⁷. The world today, in contrast, is increasingly connected, allowing diseases like Ebola⁸, Influenza^{9,10}, and COVID-19^{11,12} to spread more widely, and more quickly, than ever before.

Human movement has consequences beyond the spread of human-specific pathogens as well, being key to both the spread of wildlife-associated pathogens between otherwise isolated habitats^{13,14} and the spread of diseases between livestock populations via direct transport of infected animals¹⁵ or through contaminated vehicles or equipment¹⁶. Even in the absence of human-mediated spread, diseases in livestock and wildlife populations can have dramatic consequences on human populations through spillover, economic loss, and reduction of ecosystem services¹⁴. Thus, a better understanding of how population movement (human or otherwise) affects disease spread is critical to preventing and responding to future epidemics.

Host movement is critical both to the spread of disease across landscapes and to the persistence of pathogens in the populations they infect^{17–22}. Initially introduced through the concept of island biogeography²³, a network approach to modelling metapopulations lends itself readily to the study of empirical systems, such as human movement between cities²⁴, livestock transport between farms^{15,25}, or wildlife living in fragmented natural habitats²⁶. Representing a metapopulation of cities, for example, involves mapping each city to a node in the network and connecting those nodes with edges when there is movement of individuals between them. A network-based metapopulation framework can facilitate characterization of the relationships between connected

¹Department of Veterinary Population Medicine, University of Minnesota, St. Paul, MN, USA. ²Department of Plant Pathology, University of Minnesota, St. Paul, MN, USA. ³Department of Ecology, Evolution, and Behavior, University of Minnesota, St. Paul, MN, USA. ✉email: Michalska-Smith@pm.me

patch dynamics as well as characterize the structure of the system as a whole, providing unique insights across scales^{27,28}.

Importantly, differences in local parameter values (such as carrying capacity or transmission rate) can lead to patches within a metapopulation exhibiting disparate dynamical regimes, e.g., one patch might exhibit steady pathogen prevalence through time, while another might oscillate between high and low prevalence. These differences between patches can be particularly important when cycling or chaotic dynamics result in temporarily low local population or pathogen densities. Timely influx of individuals from asynchronous patches at such moments has the potential to rescue patches from local extinction, or provide the boost needed to ensure pathogen persistence^{26,29–33}. Moreover, understanding the dynamics of a particular patch (and its relationship to the rest of the metapopulation) is essential to developing appropriate interventions to limit further disease spread. For instance, if pathogen prevalence is cycling, timing an intervention during a lull in prevalence can improve both efficacy and cost efficiency³⁴.

The study of metapopulations has a rich and expansive history in Ecology. In the field of consumer-resource dynamics, for instance, metapopulation models have revealed the importance of spatial heterogeneity for the stability and persistence of complex ecological communities, e.g., by providing prey refugia or generating an implicit density-dependence in population growth rates^{35,36}. Likewise, movement between heterogeneous patches can allow for the exchange of individuals between asynchronously varying populations, stabilizing both consumer-resource^{35,36} and disease dynamics^{37,38}. Such mechanisms have been considered as potential answers to the naturally destabilizing forces of stochasticity and time-lags that are intrinsic to empirical systems, though comprehensive analytics of such systems has been lacking³⁹.

In disease ecology and epidemiology, metapopulations have long been used to understand the spread of disease in complex population structures^{40–42}. Most commonly, models have focused on connecting patches through pathogen transmission, rather than by the explicit movement of hosts between patches^{2,43,44}, but see^{27,28,45,46}. While more mathematically tractable, this abstraction omits the effects of population shifts (i.e., changes in local demographics and population sizes resulting from the movement of individuals between patches) on the disease dynamics, including, importantly, the movement of immune individuals. Furthermore, much of the focus thus far has been on persistence, and the positive effects of movement thereupon^{35–38,47}. In contrast, categorizing the qualitative local dynamical regimes in a two-patch metapopulation of Ricker-modelled populations, excellent work by Dey et al.⁴⁸ notes that host movement can be either stabilizing or destabilizing based on the dynamics of the origin patch. In this work, we build upon prior results, focusing on the categorical disease dynamics being experienced by a given patch in the presence or absence of host movement in both small and large metapopulations. Put simply, if a disease is exhibiting oscillatory dynamics in patch *A* and steady-state dynamics in patch *B*, does movement of individuals from *A* to *B* alter dynamics in *B*? Is the effect qualitatively different if the direction of the movement were reversed?

Using a simple disease model that can intrinsically (i.e., without environmental forcing) exhibit dynamics ranging from pathogen extinction (i.e., a disease-free equilibrium), to constant prevalence through time, to cycling or chaotic fluctuations in prevalence, we characterize the effects of host movement on disease dynamics in two parts. First, we consider the effect of simulating a continuous, proportional flow of inter-patch host movement (*sensu*⁴⁵), along with disease dynamics, on artificially simplistic sub-networks constructed to exemplify key relationships between patches. These small, archetypal networks moreover serve as building blocks of larger, more complex metapopulations. We parameterize the patches in these networks to display either (A) identical or (B) disparate dynamics in the absence of host movement, and specifically look at how those dynamics might change when host movement is occurring. Finally, we consider the effect of host movement on larger, more complex metapopulation structures, in particular asking whether and how any patterns observed at small scales might affect dynamics when embedded in larger movement networks. The robustness of each result is examined by comparing multiple parameterizations of two underlying models of within-patch disease dynamics: a Susceptible-Exposed-Infectious (SEI) model⁴⁹, and a compartmental model of multi-strain disease⁵⁰. As results are qualitatively similar between model formulations, we present just one parameterization of the SEI model here and provide additional results in the Supporting Information.

Results and discussion

Archetypal sub-networks. First, we consider the case of a chain of interconnected patches which have been parameterized to display identical dynamics in the absence of host movement (i.e., individuals move from patch *A* to *B* to *C* to *D*, and all patches share the same disease parameters and initial conditions). We found that oscillations are dampened in subsequent patches relative to those in patch *A*, reducing peak pathogen prevalence (i.e., the proportion of the patch population currently infected with the pathogen; Fig. 1). This echoes results in ecological movement networks, where local population dynamics were dampened following the introduction of host movement^{47,51}, as well as work in food-webs looking at weakly coupled predator and prey oscillators⁵². As the chain of patches is lengthened, however, the change in oscillation amplitude between subsequent patches did not necessarily continue to shrink with the addition of more patches. Concurrently, we saw an increase in the correlation between neighboring patches' prevalences, the extent of which depends on the movement rate⁵³ (Supporting Information Fig. S1).

When considered in the context of larger network structures, this dampening of oscillations suggests that prevalence in “source” patches (i.e., patches with only emigration) will tend to have greater variability as well as greater asynchrony with neighboring patches. Taken together, these pose an interesting tradeoff: at the patch level, the reduction in oscillation amplitude is generally viewed as stabilizing⁴⁹, thus increasing the likelihood of pathogen endemicism. At the same time, the increase in synchrony between patches can be destabilizing at the

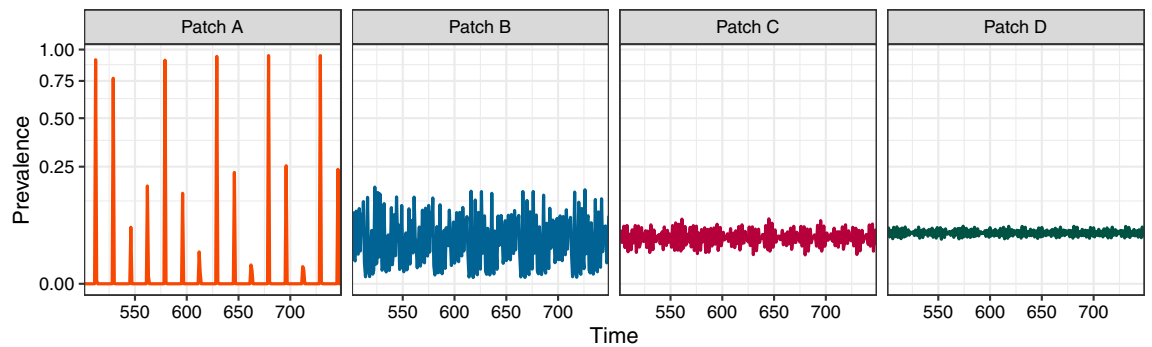


Figure 1. Connecting multiple patches with the same parameters and initial conditions results in reduced peak pathogen prevalence and dampened oscillations in patches further down the chain. Here, patches are connected such that $A \rightarrow B \rightarrow C \rightarrow D$. Each panel indicates the prevalence (i.e., the proportion of the patch population currently infected with the pathogen) over time in that particular patch. Because all patches have the same parameters and initial conditions (see Methods), all patches would have the same dynamics (i.e., cycles, as seen in⁴⁹) in the absence of movement between patches. Thus, all differences between patch time series are due to immigration from and emigration to other patches in the chain. Note also that completing the circle (such that $A \rightarrow B \rightarrow C \rightarrow D \rightarrow A$) would again make all patches identical, removing any distinction between origin and destination patches. Transient dynamics are omitted from the time series for clarity.

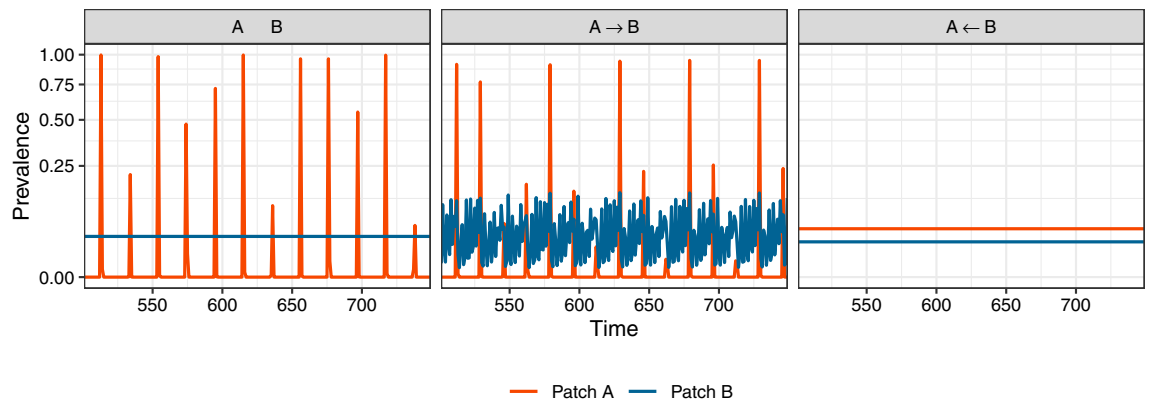


Figure 2. Destination patches tend to inherit origin patch dynamics when linking patches with different model parameterizations. Panels correspond to network structure, with line color indicating the prevalence (i.e., the proportion of the patch population currently infected with the pathogen) through time in particular patches. While in isolation (left column), patch A has oscillatory dynamics and patch B has steady-state dynamics (see Methods), when the two patches are linked by movement, the destination patch inherits the dynamics of the origin patch (center and right panels). This is true regardless of the direction of the movement (but does depend on the rate of movement; see Supporting Information Fig. S4). Transient dynamics are omitted from the time series for clarity.

metapopulation level, increasing the risk of pathogen extinction in low-prevalence patches when neighboring patch prevalence is also low^{54–56}.

Next, we consider a case in which patches are not equivalent (i.e., parameters differ between patches such that they exhibit distinct dynamical regimes in the absence of movement). When patches with disparate parameters (and thus dynamical regimes) are linked, the dynamics of destination patches can be overridden by the dynamics of origin patches (Fig. 2). While the introduction of oscillations to a steady-state patch might be expected, surprisingly, we found the opposite to also be true (i.e., steady-state dynamics overruling oscillations), though this requires a higher rate of movement (Supporting Information Fig. S4). Indeed, the cessation of oscillatory behavior, also termed “amplitude death,” has been observed even in the case of linking two entities experiencing cycling dynamics to one another^{57–60}, though most of these studies consider the effect on the system as a whole (the entire metapopulation, in our case), rather than the effects on individual entities/patches.

Because we saw both oscillatory and steady-state dynamics propagating through the metapopulation, it is natural to ask what destination dynamics look like when there are multiple, varied origin patches for a single destination patch. In such cases, we observed a hierarchy of dynamics in regard to their propagation through the network: when there are origin patches with both oscillatory and steady-state dynamics, the destination patch inherited the oscillatory dynamics, albeit dampened from what they would have been without movement from

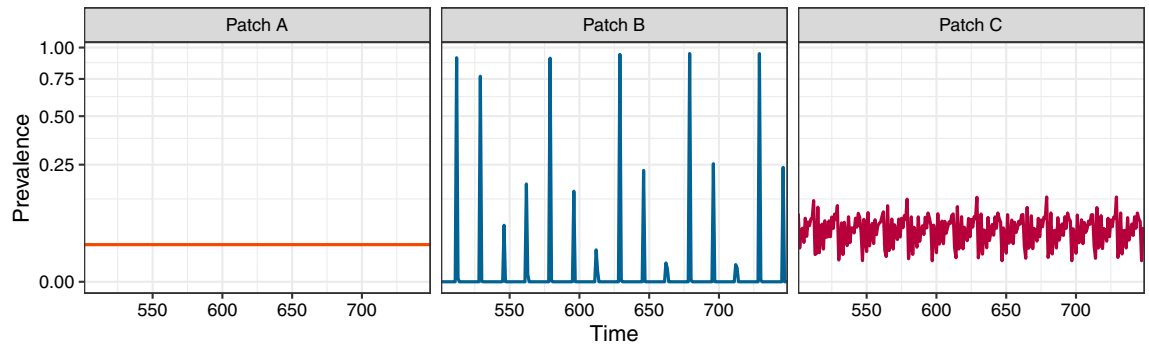


Figure 3. When multiple origin patches differ in their dynamics, the destination patch inherits oscillations over steady-states. As in Fig. 1, panels correspond to individual patches, with lines indicating the prevalence (i.e., the proportion of the patch population currently infected with the pathogen) through time. Here, we have patches *A* and *B* feeding into patch *C* at the same rate; $A \rightarrow C \leftarrow B$. *A* and *C* are parametrized to produce steady-state dynamics in the absence of movement (see Methods). *B* shows oscillatory dynamics, with all other parameters the same. Note that, even though the parameters of *C* would lead to a steady-state in the absence of movement, we see oscillatory dynamics being inherited from *B*. Transient dynamics are omitted from the time series for clarity.

a steady-state patch (Fig. 3). This asymmetrical inheritance was robust to imbalance in the relative contributions of the origins (Supporting Information Fig. S5).

The inheritance of dynamical regimes combined with a hierarchy that favors oscillatory dynamics suggests that these more volatile dynamics should be more common, especially in patches further “down the chain.” That is, except in cases where all source patches are disposed toward steady-states, in which case the stabilizing effect has the potential to overrule downstream local parameterizations, leading to an overall stable system. These results are consistent with, and provide a mechanism for, the longstanding observation that non-steady-state dynamics predominate in empirical disease systems^{61,62}, and in population dynamics more generally⁶³.

Larger network structure. Empirical networks are much larger and more connected than these simple examples—are there consequences of these local patterns on the dynamics of larger, more complex metapopulations? Rather than restricting our analysis to a small sample of empirical movement networks (few of which contain directionality or rates of movement), we evaluated the effect of various global network structures through the use of five well-studied network ensembles. Depending on the system being explored, a given empirical network might have elements in common with one or more classical network structure ensembles, for instance, many social networks are considered to be “small-world” in structure like Watts-Strogatz random networks^{64–66}, while ecological networks are often noted for their formation of “modules” or clusters of more densely interacting species as in stochastic block random networks^{67–71}. Likewise, the expected frequency of each of the aforementioned archetypal networks will vary between network ensembles, as will the ways in which these subgraphs are embedded into the wider network structure. This makes it a nontrivial question as to how, and indeed whether, the patterns observed for small networks scale up to more realistic network sizes.

While random, modular, and small-world networks all had similar distributions of dynamics across patches, with most metapopulations consisting of entirely oscillatory or entirely steady-state dynamics, tree and scale-free networks instead tended to show a diversity of dynamics across the metapopulation (Fig. 4). Network structure also varied across network types in terms of the prevalence of three-node subgraphs similar to the archetypal networks considered above. In particular, we note the frequency of in-star triads and three-node chains present in each generated network (Fig. 5). While these metrics consider network structure independent from the dynamics of disease within the composite nodes, such counts can be considered as a proxy for opportunities to observe the patterns noted in Figs. 1 to 3. Tree and scale-free networks tended to have more in-star triads (Fig. 5, again correlating with the differences in disease dynamics observed in Fig. 4 (though variance in indegree (immigration) appears to be an even better predictor of the distribution of dynamics (Supporting Information Fig. S6)).

The findings for these larger networks are in line with our predictions from the archetypal subgraphs considered earlier: as predicted, we see that patches with no immigration tend to have higher pathogen variance than patches that have at least one source of incoming host movement (Mann-Whitney $p < 0.001$), and most metapopulations show a preponderance of oscillatory behavior (Fig. 4). These results also parallel findings of increased epidemic size in scale-free network structures due to the high-degree nodes serving as “super-spreaders” when the overall rate of spread is sufficiently slow^{72–75}. Along these lines, there has been some previous research indicating that node degree is directly related to pathogen prevalence in that focal patch⁷⁶, but see⁷⁷. To our knowledge, however, no previous study has considered the distribution of qualitative local dynamical regimes across a metapopulation of more than two patches⁴⁸. A comprehensive investigation of the role of more complex network structures in disease dynamics remains a topic for further investigation.

Future directions. In probing the relationship between origin and destination dynamics in simple metapopulations, we demonstrated several patterns that expand our understanding of disease dynamics. By directly

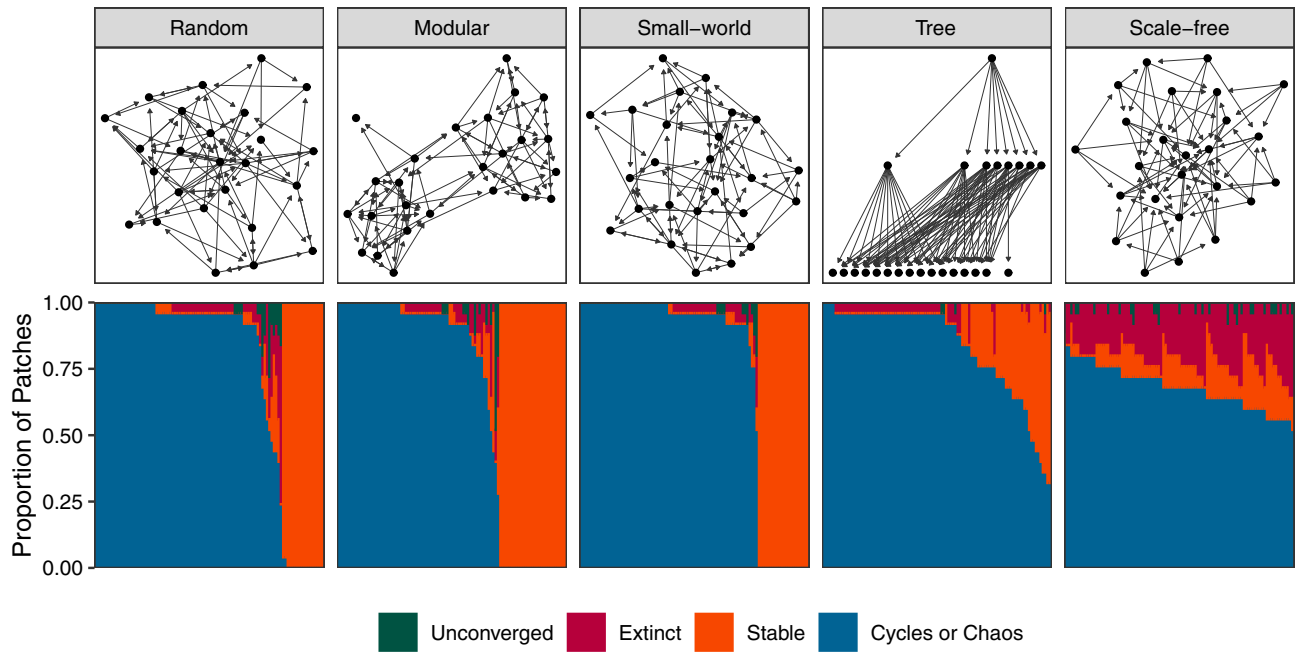


Figure 4. The proportion of patches exhibiting each dynamical regime in each of 100 random networks per network structure ensemble. Each panel shows stacked bar charts, with networks lined up along the horizontal axis, sorted according to the proportion of patches exhibiting oscillatory dynamics. Each bar is colored according to the equilibrium dynamical regime of each of the 25 patches per network. “Extinct” indicates a disease-free equilibrium for that patch, “Stable” indicates a constant prevalence through time, and “Cycles or Chaos” indicates that the prevalence fluctuates through time. “Unconverged” indicates patch dynamics that could not be classified within the timescale of the simulation. For example, looking at the tree networks, every patch in the left-most network exhibited oscillatory dynamics, while the right most network had 18 ($\approx 75\%$) patches exhibiting “Stable” dynamics. Networks were generated according to one of five algorithms (see Methods). Similar results are obtained with alternative parameter values (Supporting Information Fig. S9).

incorporating a movement network into our model framework, we outline an approach that lends itself to arbitrarily large and complex systems. This is noteworthy, as more and more natural systems are being thought of in terms of networks of interacting components (e.g., separate species in ecological communities⁷⁸ or conspecific host individuals exchanging parasites⁷⁹). By adjusting the scale of our metapopulation, we can ask and answer different questions about the forces influencing disease dynamics. For instance, a metapopulation in which nodes represent countries and edges international travel could shed light on the role of immigration policy on disease dynamics at the national scale^{9,17,28,80}. Alternatively, a metapopulation in which the nodes are individuals and edges interpersonal interactions could be used to investigate the interdependence of within-host disease dynamics in relation to sociality^{81,82}.

Critically, our results presented here are numerical, rather than analytical. While a full analysis of the mechanisms behind the patterns observed here is still outstanding, a number of mechanisms have been identified for (de)stabilizing population dynamics in prior literature, including spatial and temporal heterogeneity, spatial aggregation, functional response type, etc.^{35,36}. Interestingly, in the results presented here, the same superficial change (host movement between patches) can be both stabilizing and destabilizing based solely on the dynamics found in the origin of the movement⁴⁸. Due to the complexity of even moderately sized metapopulations, it is difficult to generalize results from two- or three-patch metapopulations to systems of the size commonly seen in nature. Nevertheless, progress in understanding the precise, mathematical mechanisms behind the changes in dynamics noted in the archetypal cases noted here is essential to make progress on larger, more impactful systems such as the spread of disease across nations, patchy habitats, or livestock production systems.

Finally, while we consider the distribution of dynamical regimes within the network (Fig. 4), we do not explicitly consider the spatial arrangement of these dynamics in relation to one another. Are the oscillatory patches clustered within the network? Do adjacent patches share dynamics more often than would be expected? A full analysis of how dynamical regimes are positioned across network structure, and in relation to the dynamics of nearby patches is a clear next step from these analyses.

Limitations. Any theoretical study involves simplification, and several of our assumptions can be critiqued as unrealistic. One example is the assumption of continuous movement. While continuous movement might be appropriate for very large patches with frequent, relatively small movements between them, when any of these three components is not present, we would expect deviation from these predictions. Future work could explore the importance of discrete movement regimes on these patterns.

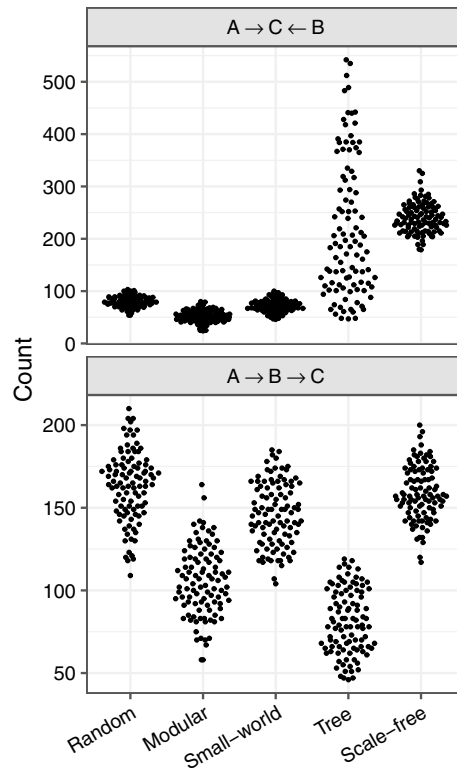


Figure 5. Triad counts for two of the possible configurations of three-node directed subgraphs in each random metapopulation network that correspond to the aforementioned archetypal networks. Points are grouped according to network structure ensemble (see Methods and top row of Fig. 4). As in Fig. 4, we see that for the “in-star” triad ($A \rightarrow C \leftarrow B$), random, modular, and small-world networks tend to have similar values, while tree and scale-free networks differ. In contrast, we see no consistency between differences in the number of chain triads ($A \rightarrow B \rightarrow C$) and the distribution of patch dynamics.

We also use a deterministic model of disease spread. The lack of stochasticity (demographic and environmental) is particularly noteworthy in the context of complex cyclical and chaotic dynamics, where population or pathogen densities occasionally recover from near infinitesimal levels. Such troughs in density are prone to stochastic extinction in real ecosystems⁴⁹. Some previous work on stochastic epidemics on metapopulations has suggested strong correlations in prevalence between connected patches⁸³, in line with our findings for connected, identical patches. While the consideration of a stochastic model is beyond the scope of this work, we highlight the need for further exploration of its impact on the patterns described here, and specifically point to the stochastic metapopulation model proposed by⁸³ as an avenue for consideration.

Another key assumption is that of unidirectional movement, despite many empirical systems having bidirectional movement (i.e., concurrent movement from $A \rightarrow B$ and movement from $B \rightarrow A$). This decision was primarily driven by the underlying theoretical question: how does movement of individuals from one patch to another alter the dynamics in the destination? With bidirectional movement, even identifying which patch is the origin and which is the destination becomes nontrivial. Yet there are also empirical systems in which directional movement is the rule, not the exception, such as in the case of livestock production⁸⁴, riverine metacommunities⁸⁵, or stage-structured populations³⁵. Several previous studies have considered bidirectional movement in metapopulation contexts^{48,57–60}, finding it to be generally stabilizing when at sufficient levels, a finding we were able to replicate in our system as well (Supporting Information Fig. S2).

Finally, even our “larger” networks are much smaller than the average empirical metapopulation. Further research is needed to explore these patterns in the context of larger and more empirically structured networks.

Conclusions. We found that the dynamics of pathogen prevalence among patches connected through movement are not independent, and that even very small rates of movement (Supporting Information Fig. S4) can have profound effects on local disease dynamics: from reducing pathogen prevalence to changing the dynamical regime of destination patches entirely. When patches that would exhibit different dynamical regimes are linked, destination patches tend to adopt the dynamics of their origins. Remarkably, given sufficient host movement, this effect is symmetric: oscillatory prevalence can be stabilized by movement from a steady-state patch and the steady-state patch can be driven into cyclical or chaotic behavior if that movement is reversed. Unsurprisingly, the latter is easier to obtain, being both able to persist at lower rates of host movement and dominating over movement from other steady-state populations when there are multiple origin patches at play. Relating the patterns observed in these archetypal patch relationships to differences that arise when considering the structure

of larger networks is nontrivial, yet we observed significant differences in the distribution of local pathogen dynamics across network types that correlate with metapopulation structure.

Critically, though we focus only on one underlying disease model⁴⁹ in the main text, our results are fully replicated under a second, independent disease model⁵⁰ in the Supporting Information Section S2. These consistent, replicated findings across parameterizations and even model frameworks suggest these patterns are inherent to pathogen spread on metapopulations, rather than merely an artifact of any particular methodological choice. While the structure of metapopulation networks can be staggeringly complex, the results presented here suggest this complexity may be undergirded with relatively simple patterns of how local disease dynamics become intertwined with one another through host movement.

Methods

Model framework. We replicate all simulations using two underlying models of disease spread: a Susceptible-Exposed-Infectious model⁴⁹, and a compartmental model of multi-strain disease⁵⁰. As results are qualitatively similar between model formulations, we present the former here and largely relegate the latter to the Supporting Information (Section S2). Importantly, we view this consistency between models as suggestive of robustness of our results to model formulation. We chose the two models detailed here and in the Supporting Information for their ability to intrinsically exhibit a wide range of dynamical regimes, including pathogen extinction, constant prevalence through time (i.e., a steady-state equilibrium), and fluctuating prevalence through time (i.e., cyclic⁴⁹ or chaotic⁵⁰ attractors).

The compartmental model described by Anderson *et al.*⁴⁹ delineates a population into classes based on their disease status, each class's dynamics being governed by an ordinary differential equation. Individuals can be either “Susceptible” to infection (S), infected but not yet infectious (i.e., “Exposed”; E), or “Infectious” (I). Infection is assumed to be lifelong and new susceptible individuals are born into the system at a constant per capita rate:

$$\begin{aligned}\frac{dS}{dt} &= rS \left(1 - \frac{N}{K}\right) - \beta SI \\ \frac{dE}{dt} &= \beta SI - \left(\sigma + \mu + r \frac{N}{K}\right)E \\ \frac{dI}{dt} &= \sigma E - \left(\nu + \mu + r \frac{N}{K}\right)I.\end{aligned}\quad (1)$$

Note that we have updated the equation lettering to reflect the modern *SIR* framework: replacing the parameter γ with the equivalent r/K , and parameters b and α with μ and ν , respectively. Thus, $N = S + E + I$ is the total host density, r is the per capita population growth rate (i.e., the difference between the per capita population birth and death rates), K is the host carrying capacity (measured as a density), β is the transmission coefficient, σ is the inverse of the average latent period, μ is the per capita death rate, and ν is the rate of disease-induced mortality. Note that this formulation assumes that only susceptible hosts reproduce.

Following⁴⁵, we modify the homogenous-population disease model using a movement matrix $\Delta = X - Y$, where X a matrix representing immigration, with X_{ij} indicating the rate of movement from patch i (row) to patch j (column) per unit time and Y is a diagonal matrix representing emigration, where each entry $Y_{ii} = \sum_{j=1}^n X_{ij}$ where n is the number of patches. The whole system can thus be depicted by a set of three equations per patch i :

$$\begin{aligned}\frac{dS_i}{dt} &= r_i S_i \left(1 - \frac{N_i}{K_i}\right) - \beta_i S_i I_i + \sum_j \Delta_{ji} S_j \\ \frac{dE_i}{dt} &= \beta_i S_i I_i - \left(\sigma_i + \mu_i + r_i \frac{N_i}{K_i}\right)E_i + \sum_j \Delta_{ji} E_j \\ \frac{dI_i}{dt} &= \sigma_i E_i - \left(\nu_i + \mu_i + r_i \frac{N_i}{K_i}\right)I_i + \sum_j \Delta_{ji} I_j\end{aligned}\quad (2)$$

Each parameter is now indexed according to its patch i . In principle, these parameters could vary between patches (e.g., one patch might grow faster than another: $r_i > r_j$), yet, for simplicity of presentation, we keep most parameters constant across the metapopulation, varying only those necessary to alter the dynamical regime between patches. For this, we focus on the patch carrying capacity K_i , which is directly associated with the dynamical regime for this system of equations⁴⁹ and is biologically realistic to vary between metapopulation patches. The rate of host movement, i.e., the elements of Δ , might likewise differ for each pair of patches (and indeed for each direction therein) in empirical systems, yet we assume a constant value δ for each rate of movement, i.e., for each non-zero off-diagonal element of Δ . Sensitivity to this value and the effects of emigration on patch dynamics are explored in the Supporting Information (Figs. S3 to S5). We follow⁴⁵ in assuming there are no births, deaths, or infections during movement between patches.

Finally, the sensitivity of results to our particular choice of parameters was assessed through replication of all results with at least two parameterizations (Supporting Information Figs. S8 and S9 and Section S2).

Simulation Procedure. As noted above, the dynamical regime exhibited by a pathogen following Eq. (1) is directly related to the host population carrying capacity K when all other parameters are held constant⁴⁹, so we restrict parameter differences between patches to differences in carrying capacity and focus on varying the

matrix Δ (i.e., the network of host movement) according to the number and pattern of connections for each patch. Expected dynamics for a homogenous population with no movement are detailed in⁴⁹.

A chain of patches, i.e., $A \rightarrow B \rightarrow C \rightarrow D$, can be depicted with the movement network

$$\Delta = \begin{array}{c} \\ A \\ B \\ C \\ D \end{array} \begin{array}{cccc} A & B & C & D \\ \left[\begin{array}{cccc} -\delta & \delta & 0 & 0 \\ 0 & -\delta & \delta & 0 \\ 0 & 0 & -\delta & \delta \\ 0 & 0 & 0 & 0 \end{array} \right] \end{array}. \quad (3)$$

We set $\delta = 0.1$ and ask how the dynamics of patches further down the chain (i.e., B, C, D) differ from those of the origin patch (i.e., A). Importantly, because we are not using a looping movement chain (in order to maintain an explicit origin and destination for each host movement), there is the possibility of edge effects (i.e., because patch A does not have any immigration and patch D does not have any emigration). The carrying capacities K are set to 15, corresponding to cyclical dynamics in the absence of host movement⁴⁹, while other parameters are set to be approximately equal to the empirical estimates in⁴⁹: $r = 0.5$, $\beta = 80$, $\sigma = 13$, $\mu = 0.5$, and $\nu = 73$, and are the same for all patches.

For patches which differ in their parameters, we consider a system of two patches, identical in all respects other than their carrying capacity K , which is set to either induce a steady-state (i.e., a constant prevalence through time; $K = 5$ in patch B) or fluctuating prevalence through time (i.e., cyclical or chaotic dynamics; $K = 15$ in patch A ; all other parameters as noted above). We then display three potential patterns of connection: no movement, unidirectional movement from A to B ($A \rightarrow B$), and unidirectional movement from B to A ($B \rightarrow A$). Specifically, we set the movement networks to be

$$\Delta = \begin{array}{c} \\ A \\ B \end{array} \begin{array}{cc} A & B \\ \left[\begin{array}{cc} 0 & 0 \\ 0 & 0 \end{array} \right], \quad \Delta = \begin{array}{c} \\ A \\ B \end{array} \begin{array}{cc} A & B \\ \left[\begin{array}{cc} -\delta & \delta \\ 0 & 0 \end{array} \right], \quad \text{and} \quad \Delta = \begin{array}{c} \\ A \\ B \end{array} \begin{array}{cc} A & B \\ \left[\begin{array}{cc} 0 & 0 \\ \delta & -\delta \end{array} \right], \end{array} \quad (4)$$

respectively.

To address the case of multiple origin patches feeding into a single destination patch, we consider a system of three patches: $A \rightarrow C \leftarrow B$, or

$$\Delta = \begin{array}{c} \\ A \\ B \\ C \end{array} \begin{array}{ccc} A & B & C \\ \left[\begin{array}{ccc} -\delta & 0 & \delta \\ 0 & -\delta & \delta \\ 0 & 0 & 0 \end{array} \right], \end{array} \quad (5)$$

where patches A and C have $K = 5$ (steady-state dynamics), but patch B has $K = 15$ (chaotic dynamics); all other parameters as above. In all cases, we assess the dynamics through consideration of the timeseries of disease prevalence, i.e., the proportion of each patch's population that is currently infected with the pathogen⁴⁹.

Larger network structure. Considering larger, more complex metapopulations, we perform 100 simulations for each of five network ensembles. For these simulations, we construct directed networks of an arbitrary size of 25 patches and connectance of approximately 0.15, but with varying network structure, according to five random-network ensembles: Erdős-Rényi-Gilbert (links randomly assigned between patches; "random"), stochastic block (two, densely connected "modules" of patches, with few inter-group connections; "modular"), Watts-Strogatz (small-world network structure produced by partially re-wiring a spatial grid of patches; "small-world"), tree-like (many chains of patches and no potential for loops, "tree"), and Barabási-Albert (scale-free degree distribution where few patches have very many links, and many patches have few links; "scale-free"). Note that we use terms like "scale-free" and "small-world" here as short-hand, bearing in mind that such structural generalizations are typically only defined in the limit of much larger network size. Network-generating algorithms from the tidygraph R package⁸⁶ were used, except for tree and Watts-Strogatz configurations which required custom algorithms. Each movement rate was set to $\delta = 0.01$, and each patch was assigned the same disease parameters as above except for carrying capacity and initial densities of susceptible, exposed, and infectious individuals, which are randomized for each patch: $K_i = [5, 20]$ and $X_i(0) = [0, 1]$, where $X \in \{S, E, I\}$ and $[a, b]$ indicates a uniformly sampled random value between a and b , inclusive.

For each network, we sought to relate properties of the network structure to the outcomes of simulated disease spread across the metapopulation. For the former, we quantified both properties of each network's degree distribution (Supporting Information Fig. S6) and the frequency of three-node subgraphs found in each network that form short chains ($A \rightarrow B \rightarrow C$; similar to the network in Eq. (3)) or in-stars ($A \rightarrow C \leftarrow B$; as used in Eq. (5)). To quantify disease outcomes, we simulated 10,000 time-steps of disease spread on each network and A) summarized pathogen prevalence over time (Supporting Information Figs. S7 and S8), and B) categorized the

dynamical regime of each patch over the final 1000 time-steps as disease-free (“Extinct”), stable pathogen prevalence (“Stable”), or fluctuating pathogen prevalence through time (“Cycles or Chaos”). Patches which could not be classified into one of these three categories within the timescale of the simulation were labeled “Unconverged” (Fig. 4, Supporting Information Fig. S9).

All numerical integrations were carried out using the DifferentialEquations package^{87,88} in Julia version 1.7.0⁸⁹, with graphics produced using the ggplot2 package⁹⁰ in R version 4.0.3⁹¹. Code can be found on GitHub: https://github.com/mjsmith037/metapop_local_dynamics.

Received: 17 November 2021; Accepted: 11 May 2022

Published online: 07 June 2022

References

- Ritchie, H. & Roser, M. Urbanization. *Our World in Data* (2018). <https://ourworldindata.org/urbanization>.
- Chen, H., Weersink, A., Beaulieu, M., Lee, Y. N. & Nagelschmitz, K. A historical review of changes in farm size in Canada. Tech. Rep., University of Guelph, Institute for the Advanced Study of Food and Agricultural Policy (2019).
- Gudelj, I. & White, K. Spatial heterogeneity, social structure and disease dynamics of animal populations. *Theor. Popul. Biol.* **66**, 139–149 (2004).
- Augustin, N., Muggleston, M. A. & Buckland, S. T. An autologistic model for the spatial distribution of wildlife. *J. Appl. Ecol.* **33**, 339–347 (1996).
- Karlsson, E. K., Kwiatkowski, D. P. & Sabeti, P. C. Natural selection and infectious disease in human populations. *Nat. Rev. Genetics* **15**, 379–393 (2014).
- Fornaciari, A. Environmental microbial forensics and archaeology of past pandemics. *Microbiol. Spect.* **5**, 5–1 (2017).
- Thèves, C., Crubézy, E. & Biagini, P. History of smallpox and its spread in human populations. *Microbiol. Spect.* **4**, 4–4 (2016).
- Coltart, C. E., Lindsey, B., Ghinai, I., Johnson, A. M. & Heymann, D. L. The ebola outbreak, 2013–2016: old lessons for new epidemics. *Philos. Trans. R. Soc. B Biol. Sci.* **372**, 20160297 (2017).
- Colizza, V., Barrat, A., Barthelemy, M., Valleron, A.-J. & Vespignani, A. Modeling the worldwide spread of pandemic influenza: Baseline case and containment interventions. *PLoS Med.* **4**, e13 (2007).
- Lüthy, I. A., Ritacco, V. & Kantor, I. N. One hundred years after the “Spanish” flu. *Medicina* **78**, 113–118 (2018).
- Zhang, Y., Zhang, A. & Wang, J. Exploring the roles of high-speed train, air and coach services in the spread of COVID-19 in China. *Transport Policy* **94**, 34–42 (2020).
- Coelho, M. T. P. *et al.* Global expansion of COVID-19 pandemic is driven by population size and airport connections. *PeerJ* **8**, e9708 (2020).
- Tompkins, D. M., Carver, S., Jones, M. E., Krkošek, M. & Skerratt, L. F. Emerging infectious diseases of wildlife: A critical perspective. *Trends Parasitol.* **31**, 149–159 (2015).
- Soulsbury, C. D. & White, P. C. Human-wildlife interactions in urban areas: A review of conflicts, benefits and opportunities. *Wildl. Res.* **42**, 541–553 (2015).
- VanderWaal, K. L. *et al.* Network analysis of cattle movements in Uruguay: Quantifying heterogeneity for risk-based disease surveillance and control. *Prevent. Vet. Med.* **123**, 12–22 (2016).
- Rossi, G. *et al.* The potential role of direct and indirect contacts on infection spread in dairy farm networks. *PLoS Comput. Biol.* **13**, e1005301 (2017).
- Stoddard, S. T. *et al.* The role of human movement in the transmission of vector-borne pathogens. *PLoS Neg. Trop. Dis.* **3**, e481 (2009).
- Cosner, C. Models for the effects of host movement in vector-borne disease systems. *Math. Biosci.* **270**, 192–197 (2015).
- Scherer, P. C. *Infection on the move: individual host movement drives disease persistence in spatially structured landscapes*. Dr. rer. nat. thesis, Universität Potsdam (2019).
- Riley, S. Large-scale spatial-transmission models of infectious disease. *Science* **316**, 1298–1301 (2007).
- Dougherty, E. R., Seidel, D. P., Carlson, C. J., Spiegel, O. & Getz, W. M. Going through the motions: Incorporating movement analyses into disease research. *Ecol. Lett.* **21**, 588–604 (2018).
- Daversa, D., Fenton, A., Dell, A., Garner, T. & Manica, A. Infections on the move: How transient phases of host movement influence disease spread. *Proc. R. Soc. B Biol. Sci.* **284**, 20171807 (2017).
- MacArthur, R. H. & Wilson, E. O. *The Theory of Island Biogeography* (Princeton University Press, 2001).
- Kobayashi, K. & Okumura, M. The growth of city systems with high-speed railway systems. *Ann. Region. Sci.* **31**, 39–56 (1997).
- VanderWaal, K., Perez, A., Torremorell, M., Morrison, R. M. & Craft, M. Role of animal movement and indirect contact among farms in transmission of porcine epidemic diarrhea virus. *Epidemics* **24**, 67–75 (2018).
- Hanski, I. Metapopulation dynamics. *Nature* **396**, 41–49 (1998).
- Colizza, V. & Vespignani, A. Epidemic modeling in metapopulation systems with heterogeneous coupling pattern: Theory and simulations. *J. Theor. Biol.* **251**, 450–467 (2008).
- Wang, L. & Li, X. Spatial epidemiology of networked metapopulation: An overview. *Chin. Sci. Bull.* **59**, 3511–3522 (2014).
- Ruxton, G. D. Low levels of immigration between chaotic populations can reduce system extinctions by inducing asynchronous regular cycles. *Proc. R. Soc. Lond. Ser. B Biol. Sci.* **256**, 189–193 (1994).
- Earn, D. J. D., Rohani, P. & Grenfell, B. T. Persistence, chaos and synchrony in ecology and epidemiology. *Proc. R. Soc. Lond. Ser. B Biol. Sci.* **265**, 7–10 (1998).
- Rosenzweig, M. L. Paradox of enrichment: Destabilization of exploitation ecosystems in ecological time. *Science* **171**, 385–387 (1971).
- Hilker, F. M. & Schmitz, K. Disease-induced stabilization of predator-prey oscillations. *J. Theor. Biol.* **255**, 299–306 (2008).
- Brown, J. H. & Kodric-Brown, A. Turnover rates in insular biogeography: Effect of immigration on extinction. *Ecology* **58**, 445–449 (1977).
- Philipson, T. Economic epidemiology and infectious diseases. *Handb. Health Econ.* **1**, 1761–1799 (2000).
- Murdoch, W. W., Briggs, C. J. & Nisbet, R. M. *Consumer-Resource Dynamics, Monographs in Population Biology* Vol. 36 (Princeton University Press, 2003).
- Murdoch, W. W. & Oaten, A. Predation and population stability. In *Advances in Ecological Research*, vol. 9, 1–131 (Elsevier, 1975).
- Bolker, B. & Grenfell, B. T. Space, persistence and dynamics of measles epidemics. *Philos. Trans. R. Soc. Lond. Ser. B Biol. Sci.* **348**, 309–320 (1995).
- Keeling, M. J. & Rohani, P. Estimating spatial coupling in epidemiological systems: a mechanistic approach. *Ecol. Lett.* **5**, 20–29 (2002).
- Arino, J. Spatio-temporal spread of infectious pathogens of humans. *Infect. Dis. Model.* **2**, 218–228 (2017).
- Keeling, M. J. & Rohani, P. *Modeling Infectious Diseases in Humans and Animals* (Princeton University Press, 2011).

41. Wilson, E. B. & Worcester, J. The spread of an epidemic. *Proc. Nat. Acad. Sci.* **31**, 327 (1945).
42. Rushton, S. & Mautner, A. The deterministic model of a simple epidemic for more than one community. *Biometrika* **42**, 126–132 (1955).
43. Lourenço, J. & Recker, M. Natural, persistent oscillations in a spatial multi-strain disease system with application to dengue. *PLOS Comput. Biol.* **9**, e1003308 (2013).
44. Wikramaratna, P. S., Pybus, O. G. & Gupta, S. Contact between bird species of different lifespans can promote the emergence of highly pathogenic avian influenza strains. *Proc. Natl. Acad. Sci.* **111**, 10767–10772 (2014).
45. Xiao, Y., Zhou, Y. & Tang, S. Modelling disease spread in dispersal networks at two levels. *Math. Med. Biol. J. IMA* **28**, 227–244 (2011).
46. Arino, J., Ducrot, A. & Zongo, P. A metapopulation model for malaria with transmission-blocking partial immunity in hosts. *J. Math. Biol.* **64**, 423–448 (2012).
47. De Roos, A. M., Mccauley, E. & Wilson, W. G. Mobility versus density-limited predator-prey dynamics on different spatial scales. *Proc. R. Soc. Lond. Ser. B Biol. Sci.* **246**, 117–122 (1991).
48. Dey, S., Goswami, B. & Joshi, A. Effects of symmetric and asymmetric dispersal on the dynamics of heterogeneous metapopulations: Two-patch systems revisited. *J. Theor. Biol.* **345**, 52–60 (2014).
49. Anderson, R. M., Jackson, H. C., May, R. M. & Smith, A. M. Population dynamics of fox rabies in Europe. *Nature* **289**, 765–771 (1981).
50. Gupta, S., Ferguson, N. & Anderson, R. Chaos persistence, and evolution of strain structure in antigenically diverse infectious agents. *Science* **280**, 912–915 (1998).
51. Holland, M. D. & Hastings, A. Strong effect of dispersal network structure on ecological dynamics. *Nature* **456**, 792–794 (2008).
52. McCann, K., Hastings, A. & Huxel, G. R. Weak trophic interactions and the balance of nature. *Nature* **395**, 794–798 (1998).
53. Singh, A. & Gakkhar, S. Synchronization of chaos in a food web in ecological systems. *World Acad. Sci. Eng. Technol.* **70**, 94–98 (2010).
54. Gotelli, N. J. Metapopulation models: The rescue effect, the propagule rain, and the core-satellite hypothesis. *American Naturalist* **138**, 768–776 (1991).
55. Heino, M., Kaitala, V., Ranta, E. & Lindström, J. Synchronous dynamics and rates of extinction in spatially structured populations. *Proc. R. Soc. Lond. Ser. B Biol. Sci.* **264**, 481–486 (1997).
56. Molofsky, J. & Ferdy, J.-B. Extinction dynamics in experimental metapopulations. *Proc. Natl. Acad. Sci.* **102**, 3726–3731 (2005).
57. Saxena, G., Prasad, A. & Ramaswamy, R. Amplitude death: The emergence of stationarity in coupled nonlinear systems. *Phys. Rep.* **521**, 205–228 (2012).
58. Majhi, S. & Ghosh, D. Amplitude death and resurgence of oscillation in networks of mobile oscillators. *Europhys. Lett.* **118**, 40002 (2017).
59. Shen, C., Chen, H. & Hou, Z. Mobility and density induced amplitude death in metapopulation networks of coupled oscillators. *Chaos* **24**, 043125 (2014).
60. Karnatak, R., Ramaswamy, R. & Feudel, U. Conjugate coupling in ecosystems: Cross-predation stabilizes food webs. *Chaos Solitons Fractals* **68**, 48–57 (2014).
61. Bolker, B. M. & Grenfell, B. T. Chaos and biological complexity in measles dynamics. *Proc. R. Soc. Lond. Ser. B Biol. Sci.* **251**, 75–81 (1993).
62. Olsen, L. F., Truty, G. L. & Schaffer, W. M. Oscillations and chaos in epidemics: A nonlinear dynamic study of six childhood diseases in Copenhagen, Denmark. *Theor. Popul. Biol.* **33**, 344–370 (1988).
63. Lundberg, P., Ranta, E., Ripa, J. & Kaitala, V. Population variability in space and time. *Trends Ecol. Evolut.* **15**, 460–464 (2000).
64. Dekker, A. Realistic social networks for simulation using network rewiring. In *International Congress on Modelling and Simulation*, 677–683 (2007).
65. Milgram, S. The small world problem. *Psychol. Today* **2**, 60–67 (1967).
66. Sallaberry, A., Zaidi, F. & Melançon, G. Model for generating artificial social networks having community structures with small-world and scale-free properties. *Soc. Netw. Anal. Min.* **3**, 597–609 (2013).
67. Olesen, J. M., Bascompte, J., Dupont, Y. L. & Jordano, P. The modularity of pollination networks. *Proc. Natl. Acad. Sci.* **104**, 19891–19896 (2007).
68. Stouffer, D. B. & Bascompte, J. Compartmentalization increases food-web persistence. *Proc. Natl. Acad. Sci.* **108**, 3648–3652 (2011).
69. Girvan, M. & Newman, M. E. Community structure in social and biological networks. *Proc. Natl. Acad. Sci.* **99**, 7821–7826 (2002).
70. Krause, A. E., Frank, K. A., Mason, D. M., Ulanowicz, R. E. & Taylor, W. W. Compartments revealed in food-web structure. *Nature* **426**, 282–285 (2003).
71. Rezende, E. L., Albert, E. M., Fortuna, M. A. & Bascompte, J. Compartments in a marine food web associated with phylogeny, body mass, and habitat structure. *Ecol. Lett.* **12**, 779–788 (2009).
72. Pastor-Satorras, R. & Vespignani, A. Epidemics and immunization in scale-free networks. In *Handbook of Graphs and Networks*, 111–130 (Wiley Online Library, 2002).
73. Lloyd-Smith, J. O., Schreiber, S. J., Kopp, P. E. & Getz, W. M. Superspreading and the effect of individual variation on disease emergence. *Nature* **438**, 355–359 (2005).
74. Shirley, M. D. & Rushton, S. P. The impacts of network topology on disease spread. *Ecol. Complex.* **2**, 287–299 (2005).
75. Keeling, M. J. & Eames, K. T. Networks and epidemic models. *J. R. Soc. Interface* **2**, 295–307 (2005).
76. Godfrey, S. S., Bull, C. M., James, R. & Murray, K. Network structure and parasite transmission in a group living lizard the gidgee skink, *Egernia stokesii*. *Behav. Ecol. Sociobiol.* **63**, 1045–1056 (2009).
77. VanderWaal, K. L., Atwill, E. R., Hooper, S., Buckle, K. & McCowan, B. Network structure and prevalence of *Cryptosporidium* in Belding's ground squirrels. *Behav. Ecol. Sociobiol.* **67**, 1951–1959 (2013).
78. Proulx, S. R., Promislow, D. E. & Phillips, P. C. Network thinking in ecology and evolution. *Trends Ecol. Evolut.* **20**, 345–353 (2005).
79. Craft, M. E. & Caillaud, D. Network models: An underutilized tool in wildlife epidemiology?. *Interdiscip. Perspect. Infect. Dis.* 2011, (2011).
80. Bajardi, P. *et al.* Human mobility networks, travel restrictions, and the global spread of 2009 h1n1 pandemic. *PloS one* **6**, e16591 (2011).
81. Gog, J. R. *et al.* Seven challenges in modeling pathogen dynamics within-host and across scales. *Epidemics* **10**, 45–48 (2015).
82. Cen, X., Feng, Z. & Zhao, Y. Emerging disease dynamics in a model coupling within-host and between-host systems. *J. Theor. Biol.* **361**, 141–151 (2014).
83. Meakin, S. R. & Keeling, M. J. Correlations between stochastic epidemics in two interacting populations. *Epidemics* **26**, 58–67 (2019).
84. Machado, G. *et al.* Identifying outbreaks of porcine epidemic diarrhea virus through animal movements and spatial neighborhoods. *Sci. Rep.* **9**, 1–12 (2019).
85. Tonkin, J. D. *et al.* The role of dispersal in river network metacommunities: Patterns, processes, and pathways. *Freshwater Biol.* **63**, 141–163 (2018).
86. Pedersen, T. L. *tidygraph: a tidy API for graph manipulation* (2019). R package version 1.1.2.
87. Rackauckas, C. & Nie, Q. *Differentialequations.jl—a performant and feature-rich ecosystem for solving differential equations in Julia*. *J. Open Res. Softw.* **5** (2017).

88. Rackauckas, C. & Nie, Q. Confederated modular differential equation APIS for accelerated algorithm development and benchmarking. *Adv. Eng. Softw.* **132**, 1–6 (2019).
89. Bezanson, J., Edelman, A., Karpinski, S. & Shah, V. B. Julia: A fresh approach to numerical computing. *SIAM Rev.* **59**, 65–98 (2017).
90. Wickham, H. *ggplot2: Elegant Graphics for Data Analysis* (Springer, 2016).
91. R Core Team. *R: A language and environment for statistical computing*. R Foundation for Statistical Computing, Vienna, Austria (2020).

Acknowledgements

We would like to thank Montserrat Torremorell and Cesar Corzo for conceptual discussions and feedback on early drafts of this work, as well as José Lourenço for helpful methodological discussions. This work was supported by the CVM Research Office UMN Ag Experiment Station General Research Funds, National Science Foundation DEB-2030509, and a UMN Office of Academic Clinical Affairs COVID-19 Rapid Response Grant.

Author contributions

M.M. conceived the project, performed simulations, generated figures, and wrote the draft. K.V. edited the draft and helped with conceptualization. M.E.C. supervised the project, edited the draft, and helped with conceptualization.

Competing interest

The authors declare no competing interests.

Additional information

Supplementary Information The online version contains supplementary material available at <https://doi.org/10.1038/s41598-022-12774-5>.

Correspondence and requests for materials should be addressed to M.M.-S.

Reprints and permissions information is available at www.nature.com/reprints.

Publisher's note Springer Nature remains neutral with regard to jurisdictional claims in published maps and institutional affiliations.



Open Access This article is licensed under a Creative Commons Attribution 4.0 International License, which permits use, sharing, adaptation, distribution and reproduction in any medium or format, as long as you give appropriate credit to the original author(s) and the source, provide a link to the Creative Commons licence, and indicate if changes were made. The images or other third party material in this article are included in the article's Creative Commons licence, unless indicated otherwise in a credit line to the material. If material is not included in the article's Creative Commons licence and your intended use is not permitted by statutory regulation or exceeds the permitted use, you will need to obtain permission directly from the copyright holder. To view a copy of this licence, visit <http://creativecommons.org/licenses/by/4.0/>.

© The Author(s) 2022